Vector-valued Probabilistic Seismic Demand Assessment of Structures under Two-Component Ground Motions

Salar Manie[1], Abdolreza S. Moghadam[2*], and Mohsen Ghafory-Ashtiany[3]

1. Department of Civil Engineering, Science and Research Branch, Islamic Azad University, Tehran, Iran
2. Associate Professor, Structural Earthquake Engineering Department, IIEES, Tehran, Iran, * Corresponding Author; email: moghadam@iiees.ac.ir
3. Professor, Structural Earthquake Engineering Department, IIEES, Tehran, Iran

Received: 06/04/2014
Accepted: 20/05/2014

ABSTRACT

The present paper is an attempt to quantify probabilistic seismic demand of three-dimensional structures under two-component (vector-valued) ground motions, focusing on the collapse region of nonlinear response. While utilizing results of de-aggregated vector-valued probabilistic seismic hazard analysis (V-PSHA) as the seismic demand input, the assessment procedure is essentially based on results of nonlinear incremental dynamic analysis (IDA) of the three-dimensional (3D) model of the structure. Response of the structure is formulated based on the SRSS combination of the structure maximum inter-story drifts in plan orthogonal directions assuming log-normal distribution of the demands. The efficiency of the proposed procedure is demonstrated via a detailed step-by-step example with different period of vibrations and structural properties in orthogonal directions, which proves the adequacy of the method for practical vector-valued probabilistic seismic evaluation of regular and irregular structures.

Keywords:
Vector-valued seismic demand assessment; Probabilistic; Performance-based design; Collapse; Intensity measure; IDA

1. Introduction

Proper estimation of seismic risk to a structure requires the consideration of both ground motion hazard, to which the structure is exposed, and the effect of such motions on the response of the structure. The hazard is typically provided by seismologists with the assessment of the effects of ground motions on structures being a task conducted by engineers. The structural response parameter is usually referred to as "Engineering Demand Parameter (EDP)", while the selected ground motion intensity parameter is referred to as "Intensity Measure (IM)" [1]. In probabilistic performance-based seismic assessment procedures, selection of an appropriate IM along with proper estimation of structural responses as a function of the selected IM plays a key role.

Various EDPs and IMs have been proposed so far; all have their own advantages and disadvantages in terms of accuracy, efficiency, sufficiency, and practical possibilities [2-4]. Generally, it has been shown in past studies (e.g. [2, 5, 6] that vector-valued IMs consisting of multiple spectral accelerations at different periods are sufficient and more efficient predictors of the structural response, and therefore provide more reliable seismic demand assessments.

A majority of past IDA-based studies on probabilistic seismic assessment have primarily tended to

focus on using single-valued IM, typically chosen to be the spectral ordinate at the fundamental period of the structure in its own plane (S_{a-T1}) [1, 7] or vector-valued IMs [2] in two dimensional (2D) structural frames.

Owing to the fact that real structures respond in a 3D sense and typically simple and, at the same time, accurate representation of structures, especially those with correlated orthogonal responses (such as plan-asymmetric structures) via a 2D model is generally not possible. The case would be much more critical while considering the collapse region of nonlinear response, it is necessary to deal with the problem from a 3D point of view. Barbosa [6] and Faggella et al. [8] utilized vector-valued IMs in combination with cloud analysis results to assess seismic demands of 3D structures without directly accounting for post-peak and near-collapse regions of response. Gehl et al. [9] studied the fragility (in terms of probability of collapse) of a 3D masonry structure by incorporating vector-valued PGA-PGV representation of seismic demands. Their work was also based on cloud analysis method. Many previous investigations of vector-valued IMS have been based on results of the cloud analysis method rather than the results of incremental dynamic analysis (IDA) [5].

The present paper is an attempt to quantify probabilistic seismic demand of three-dimensional structures under two-component (vector-valued) ground motions considering the collapse region of nonlinear response. In this regard, a vector-valued IM, consisting of spectral ordinates at the fundamental periods of the structure in orthogonal horizontal directions (vertical component of the ground motion is not considered in this study) is employed along with the results of incremental dynamic analysis (IDA) of the 3D model of the structure with special attention to the near-collapse region of response. The efficiency of the procedure in practical applications is demonstrated via a step-by-step example for a typical 3D reinforced concrete (RC) structure with different period of vibrations and stiffness and strength characteristics in orthogonal directions.

2. Estimation of Seismic Demands Using Scalar-Valued IMs

In scalar probabilistic seismic demand analysis (PSDA), the "demand side" of the problem is usually expressed in the form of annual rate of exceedance an EDP for a specified level of ground motion intensity (typically chosen to be the spectral intensity at the fundamental period of vibration of the structure (S_{a-T_1})). The final results is usually represented as the EDP hazard curve [1]. This curve is calculated on the basis of the following expression for any intensity-measure (*im*) value:

$$\lambda_{EDP}(d) = \int_x P[EDP > d \,|\, IM = x] \,|\, d\lambda_{IM}(x)| \qquad \text{(1-a)}$$

where $\lambda_{EDP}(d)$ is the annual rate of exceedance the desired EDP (usually maximum inter-story drift) from a certain "*d*" value $P[EDP > d \,|\, IM = x]$ is the probability that the EDP exceeds "*d*" given any known IM (for example S_{a-T_1}) and $\lambda_{IM}(x)$ is the mean annual frequency of exceeding the IM from a given intensity level "*x*". Numerical solution techniques exist to solve the integral in Eq. (1-a); however, under appropriate assumptions, closed-form solution approaches are also possible [1]. The above-mentioned approach is, indeed, an IM-based one. Assuming that the displacement-based demand has a lognormal distribution at each S_a level, $P[EDP > d \,|\, IM = x]$ can be replaced by a standardized Gaussian complementary cumulative density function (CCDF) (F^C) [10] as follows:

$$\lambda_{EDP}(d) = \int_x \{F^c(d \mid x)\}.|\, d\lambda_{IM}(x) \Big| = \int_x \{1 - F(d \mid x)\}.|\, d\lambda_{IM}(x)\Big| \qquad \text{(1-b)}$$

where "F" denotes the Gaussian cumulative density function.

In order to take the collapse-level cases of structural response into account, the conditional probability $P[EDP > d \,|\, IM = x]$ can be decomposed into non-collapse and collapse cases using the total probability theorem (TPT) [2, 11] as Eq. (2). Note that in Eq. (2), EDP and IM have been replaced by the maximum inter-story drift ($D_{\max}$) observed in the structure and the spectral intensity at the fundamental period of vibration of the structure (S_{a1}), respectively:

$$\begin{aligned} &P[D_{\max} > d \mid S_a = x] = \\ &F^c_{D_{\max}|NCL}(d \mid x).P_{NCL|S_a}(x) + \\ &F^c_{D_{\max}|CL}(d \mid x).(1 - P_{NCL|S_a}(x)) \end{aligned} \qquad \text{(2)}$$

where $P_{NCL|S_a}(x)$ is the probability of no-collapse for a given spectral level "x" and $(1-P_{NCL|S_a}(x))$ is the probability of collapse for the same spectral level, x). Probability of no-collapse and collapse can be derived directly from the data provided by the IDA analysis results. Such Methods have been discussed in [1-2]. Regarding the collapse cases, the probability that the demand ($D_{\max}$) exceeds any finite drift, d, $F^{c}_{D_{\max}|NCL}(d \mid x)$ is equal to 1; thus Eq. (2) can be reduced to Eq. (3) as:

$$P[D_{\max} > d \mid S_a = x] = F^{c}_{D_{\max}|NCL}(d \mid x).P_{NCL|S_a}(x) + (1-P_{NCL|S_a}(x)) \quad (3)$$

By substitution of Eq. (3) with Eq. (1-a) and integrating, one can estimate the annual probability of exceeding any drift value d taking the collapse region of nonlinear response into consideration. Note that the above process of determining non-collapse and collapse cases is limited to scalar-valued IM (S_a).

Baker and Cornell [2] extended Eq. (1-a) to include a vector-valued IM consisting of S_a and a random variable "ε" value, representative of spectral shape of the ground motion.

3. Estimation of Structural Response of 3D Structures Using Vector-Valued IMs

In this study, the demand side of the problem has been considered to be the SRSS combination of horizontal orthogonal inter-story drift values as a representative of the seismic demands on each story of the 3D structure. Considering the maximum inter-story demands for 3D structures as the SRSS combination of horizontal directions drifts conditioned on bi-directional IMs, namely S_{aX} and S_{aZ} (note that for brevity, $S_{a(T1-i)}$ has been replaced by S_{ai} and y-direction is assumed to direct upward), Eq. (1-a) can be rewritten using a vector-valued IM as:

$$\lambda_{EDP}(D) = \int_x^{\partial}\int_z^{\partial} P[D_{\max-SRSS} > D \mid S_{aX} = x,\ S_{aZ} = z] \times \left|\frac{\partial^2 \lambda_{IM-X,Z}}{\partial x \partial z}\right| dx\,dz \quad (4)$$

where $D_{\max-SRSS}$ denotes the maximum *SRSS* combination of maximum inter-story drifts observed along orthogonal plan directions, S_{aX} and S_{aZ} represent the spectral intensity levels at the fundamental periods of vibration along X and Z directions, respectively. Besides, $\left|\frac{\partial^2 \lambda_{IM-X,Z}(x,z)}{\partial x \partial z}\right|$ denotes the absolute value of the second-order derivative of the vector-valued hazard $\lambda_{IM-X,Z}(x,z)$ (at each $S_{aX} = x$, $S_{aZ} = z$ pairs, in this study) for a specific site; to be obtained based on a probabilistic vector-valued seismic hazard analysis (V-PSHA). In discrete form, Eq. (4) can be written as Eq. (5), which is appropriate for numerical integration:

$$\lambda_{EDP}(D) \cong \sum_{all\ x}\sum_{all\ z} \times P[D_{\max-SRSS} > D \mid S_{aX} = x, S_{aZ} = z] \times |D\lambda_{IM-X,Z}(x,z)| \quad (5)$$

The conventional product of PSHA is typically a scalar-valued "hazard curve" rather than a vector-valued "hazard surface". For our purpose, bi-directional (joint) representation of the seismic hazard (at each $S_{aX} = x$, $S_{aZ} = z$ pairs)) is needed. Such representation, introduces a "seismic hazard surface" rather than the conventional "seismic hazard curve" ([12-14]. The issue of vector-valued seismic hazard analysis with its implications in practical seismic design has been discussed before [15-19].

Although utilization of vector-valued seismic hazard surface (defined by $(\lambda_{IM-X,Z}(x,z))$ in Eq. (5)) is quite straightforward, due to the limitations in accessing the few available computer codes for generating such joint seismic hazard surfaces and their documentations on the one hand, and the unavailability of statistical correlation coefficients for all types of IMs, on the other, reformulating Equation (5) by means of de-aggregating the joint seismic hazard function into scalar functions and utilizing the widely available scalar probabilistic seismic hazard analysis results has become a standard procedure in vector-valued probabilistic seismic demand analysis (V-PSDA) studies [6].

By disaggregating the $D\lambda_{IM-X,Z}(x,z)$ term in Eq. (5) using the definition of conditional probability, Eq. (6) can be derived:

$$D\lambda_{IM-X,Z}(x,z) = P(S_{aZ} = z \mid S_{aX} = x).D\lambda_{SaX}(x) \quad (6)$$

By replacing Eq. (6) with Eq. (5) and using the assumption that the drift demands follow a log-normal distribution (This assumption could be verified by statistical testing methods. For this study, the authors have used two "normality tests" developed by Doornik and Hensen [20], and Henze and Zirkler [21] to verify the normality. Multivariate normality of the natural logarithm of spectral accelerations at multiple periods has also been empirically tested by Jayaram and Baker [4]), one can rewrite Eq. (5) as:

$$\lambda_{EDP}(D) \cong \sum_{all\ x}\sum_{all\ z}\{1-F^{\,c}_{D_{\max-SRSS}} \times (D \mid x,z)\}P(S_{aZ}=z \mid S_{aX}=x)\times \mid D\lambda_{SaX}(x)\mid = \sum_{all\ x}\sum_{all\ z}\{F^{\,c}_{D_{\max-SRSS}}(D \mid x,z)\}\times P(S_{aZ}=z \mid S_{aX}=x)\times \mid D\lambda_{SaX}(x)\mid \quad (7)$$

where,

$$F^{\,c}_{D_{\max-SRSS}}(D \mid x,z) = 1-F^{\,c}_{D_{\max-SRSS}}(D \mid x,z) \quad (8)$$

By further de-aggregating the problem to take no-collapse and collapse cases into account, similar to Eq. (3) for scalar IM cases, Eq. (9) can be established as the general formulation for estimating the maximum inter-story drifts (in terms of SRSS combination) throughout the structure by considering the simultaneous effects of orthogonal horizontal components of ground motions and the collapse region of nonlinear response:

$$\sum_{all\ x}\sum_{all\ z}\{\left[F^{\,c}_{D_{\max-SRSS}}(D|x,z)P_{NCL|S_{aX},S_{aZ}}(x,z)\right] + \left[1-P_{NCL|S_{aX},S_{aZ}}(x,z)\right]\}\times P(S_{aZ}=z \mid S_{aX}=x)\times \mid D\lambda_{SaX}(x)\mid \quad (9)$$

The terms $F^{\,c}_{D_{\max-SRSS}|NCL}(D \mid x,z)$ and $P_{NCL|S_{aX},S_{aZ}}(x,z)$ are calculated using results of IDA analysis of the 3D model of the structure under simultaneous application of horizontal components of ground motion, the term $P(S_{aX}=x \mid S_{aZ}=z)$ is estimated as discussed below, and, finally, $\mid D\lambda_{SaX}(x)\mid$ is calculated as the absolute form of the values of conventional scalar probabilistic seismic hazard analysis at specific $S_{aX}=x$ values.

Barbosa [6] has discussed in detail the numerical calculation of $P(S_{aZ}=z \mid S_{aX}=x)$ for each $P(S_{aX}=x \mid S_{aZ}=z)$ pairs. This term is calculated as:

$$P(S_{aZ}=z \mid S_{aX}=x) = \sum_{all\ m}\sum_{all\ r}P(S_{aZ}=z \mid S_{aX}=x,m,r)\times P(m,r \mid S_{aX}=x) \quad (10)$$

in which m and r denotes the events magnitude and distance to the fault, respectively. In Eq. (10), $P(S_{aZ}=z \mid S_{aX}=x,m,r)$ can be evaluated for each triple $S_{aX}=x,m,r)$ as derived by Barbosa [6]:

$$P(S_{aZ}=z \mid S_{aX}=x,m,r) = F\left(\frac{\ln\left(\frac{z+Dz}{2}\right)-\mu_{\ln(S_{aZ}=z|S_{aX}=x,m,r)}}{\sigma_{\ln(S_{aZ}=z|S_{aX}=x,m,r)}}\right) - F\left(\frac{\ln\left(\frac{z-Dz}{2}\right)-\mu_{\ln(S_{aZ}=z|S_{aX}=x,m,r)}}{\sigma_{\ln(S_{aZ}=z|S_{aX}=x,m,r)}}\right) \quad (11)$$

where F is the standard normal CDF of the argument, and $\mu_{(.)}$ and $\sigma_{(.)}$ correspond to the conditional mean and conditional standard deviation defining the conditional probability density function (PDF) of $S_{aZ}=z$ given $S_{aX}=x,m,r$. Moreover D is the discretization step of spectral accelerations used in the analysis. The conditional $\mu_{\ln(S_{aZ}=z|S_{aX}=x,m,r)}$ and $\sigma_{\ln(S_{aZ}=z|S_{aX}=x,m,r)}$ can also be calculated using the following equations [5-6]:

$$\mu_{\ln(S_{aZ}=z|S_{aX}=x,m,r)} = \tilde{\mu}_{\ln(S_{aZ}=z|m,r)} + \rho_{\ln(S_{aX}=x,S_{aZ}=z)}\frac{\tilde{\sigma}_{\ln(S_{aZ}=z|m,r)}}{\tilde{\sigma}_{\ln(S_{aX}=x|m,r)}}\times [\ln(S_{aX}=x)-\tilde{\mu}_{\ln(S_{aX}=x|m,r)}] \quad (12\text{-a})$$

$$\sigma_{\ln(S_{aZ}=z|S_{aX}=x,m,r)} = \tilde{\sigma}_{\ln(S_{aZ}=z|m,r)}\sqrt{1-\left[\rho_{\ln(S_{aX}=x,S_{aZ}=z)}\right]^2} \quad (12\text{-b})$$

In Eqs. (12-a) and (12-b), $\tilde{\mu}$ and $\tilde{\sigma}$ are the mean and standard deviation of scalar spectral accelerations, calculated by using ground motion prediction equations (GMPEs), and ρ denotes the statistical correlation coefficient of the two spectral ordinates corresponding to the fundamental periods of vibration of the structure in horizontal orthogonal directions.

In this study, for the sample structure (to be discussed later), the average of three GMPEs available in NGW program (PEER), including the Abrahamson and Silvia [14], Boore and Atkinson [22], and Campbell and Bozorgnia [23] have been used with equal weights to calculate $\tilde{\mu}$ and $\tilde{\sigma}$ for each spectral period. Besides, for calculation of the correlation coefficients of spectral ordinates at the fundamental periods of vibration of the structure in horizontal orthogonal directions ($\rho_{\ln(S_{aX}=x,S_{aZ}=z)}$), Eq. (13) according to Baker and Jayaram [24] was used:

$$\rho_{\ln(S_{aX}=x,S_{aZ}=z)} = 0.79 - 0.023\ln(\sqrt{T_1 T_2}) \qquad (13)$$

where T_1 and T_2 denotes the fundamental periods of vibration of the structure in horizontal orthogonal directions.

The second term ($P(m,r \mid S_{aX}=x)$) in Eq. (10), needs to be evaluated using standard hazard de-aggregating procedure. Results of such procedure for specific spectral periods are accessible via an online interactive computer program developed by United States Geological Survey [25]. Figure (1) depicts one of such results for a specific site (considered for the example problem of this paper) at $T=1$ sec and 2% probability of exceedance in 50 years hazard level. Outputs of the program are, in fact, the contribution of each pair of magnitude (m) and distance-to-fault (r) to the total hazard under specific conditions. The outputs provided by USGS essentially gives the probability of $P(m,r \mid S_{aX} > x)$ and not exactly the $P(m,r \mid S_{aX} = x)$. Thus, for our purposes $P(m,r \mid S_{aX} = x)$, need to be calculated according to Eq. (14) [6]:

$$P(m,r \mid S_{aX} = x) = \frac{P(m,r \mid S_{aX} > x - Dx).P(S_{aX} > x - Dx)}{P(S_{aX} > x - Dx) - P(S_{aX} > x + Dx)} - \frac{P(m,r \mid S_{aX} > x + Dx).P(S_{aX} > x + Dx)}{P(S_{aX} > x - Dx) - P(S_{aX} > x + Dx)} \qquad (14)$$

4. Example Problem: Step-by-Step Procedure for Calculating the Seismic Demand of a Plan Asymmetric 3D Structure Using a Two-Component (Vector-Valued) Intensity Measure (IM)

Based on the procedure presented in previous sections, a three-dimensional structure will be

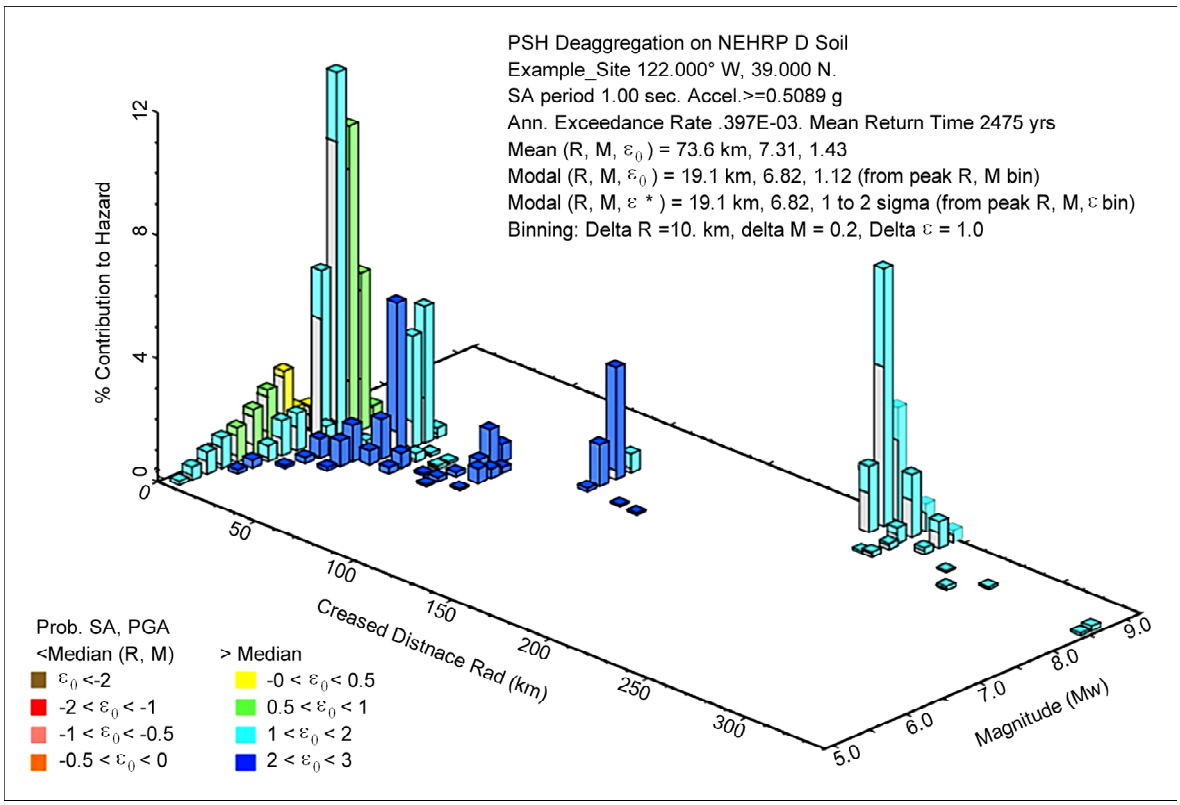

Figure 1. Probabilistic seismic hazard de-aggregation for a typical site, $IM = S_a(T = 1 \text{ sec})$, and 2% in 50 years (2475 years return period) hazard level [25].

examined to show the required steps for calculating the drift hazard, λ_{EDP}, considering the collapse region of nonlinear response. Later, more detailed discussions will be provided.

4.1. Problem Definition

The structure is a 6-story 3-span by 3-span reinforced concrete (RC) structure designed according to International Building Code [26] provisions. Reinforcements detailing conforms to the ACI code [27] requirements for "special moment resisting frames". Span lengths are identical in both directions equal to 5 meters and story heights are considered to be of 3-meter high. Floor system is considered as one-way reinforced concrete slab system. Columns are 450 mm square sections in stories 1 to 4, and are 400 mm in stories 5 and 6, while beams have 450 mm width and 500 mm height in stories 1 to 3, and have 400 mm width and 450 mm height in stories 4 to 6. Distributed dead and live loads on floors are 5.3 kN/m^2 and 2 kN/m^2, respectively. Concrete 28-day cylindrical specified strength and rebar strength are assumed to be 30 MPa and 400 MPa, respectively. Floor slab are assumed to be rigid in their plane.

In order to make the orthogonal responses of the structure quite correlated, uni-directional plan eccentricity equal to 30% was imposed between the center of mass (CM) and the center-of-stiffness (CR) via displacing the CM of each floor along the X-direction of plan. Fundamental periods of vibrations of the structure are $T_1 = 1.87$ sec. and $T_2 = 0.96$ sec. along the Z and X plan directions, respectively. Due to the strong torsional effects and the direction of transferring floor loads to the supporting frames, reinforcements in the Z-direction beam elements are typically around two times their X-direction counterparts. Thus, the structure is plan-asymmetric with highly correlated orthogonal properties. Figure (2) shows typical stories plan of the structure. We are going to estimate the annual rate of exceedance specific inter-story drift value (in SRSS sense) in the structure using the procedure discussed in previous sections.

4.2. Nonlinear Modeling and Analyzing the Structure

For performing nonlinear analyses, the structural system was modeled using concentrated plasticity

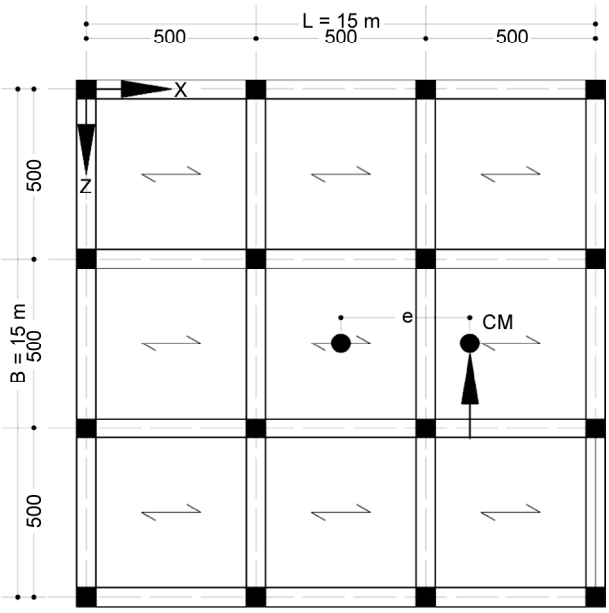

Figure 2. Typical stories plan (The eccentricity "e" for the example problem is set to be 0.3 L).

nonlinear modeling approach [28], in which hinges are modeled and defined at the ends of each frame element. As discussed in [29-3], concentrated plasticity models could be used for collapse-state analysis of structures by considering all degradation sources including the loading and reloading stiffness, peak-strength and hardening zone stiffness degradation effects in each cycle of response. Ibarra et al. [31] proposed a hysteretic model, based on the kinematic hardening rules, applicable for nonlinear modeling of RC structures to assess their collapse behavior. The model known as "peak-oriented hysteretic model" is depicted in Figure (3). All required parameters to define the elastic, peak and post-peak response of elements under monotonic and cyclic behaviors were calculated according to the design properties of the structure [32] and the recommendations of FEMA [28], Haselton [30] and Ibarra and Krawinkler [33].

The model was built in OpenSees platform [34] by using CECARC-3D; a graphical pre- and post-processor for OpenSees designed by the authors for modeling and analyzing nonlinear static and dynamic response of 3D reinforced concrete structural systems [35]. Elastic analyses of all models were performed using appropriate cracked section properties based on recommendations outlined in FEMA P-695. According to FEMA P-695, since all formulas have been derived based on

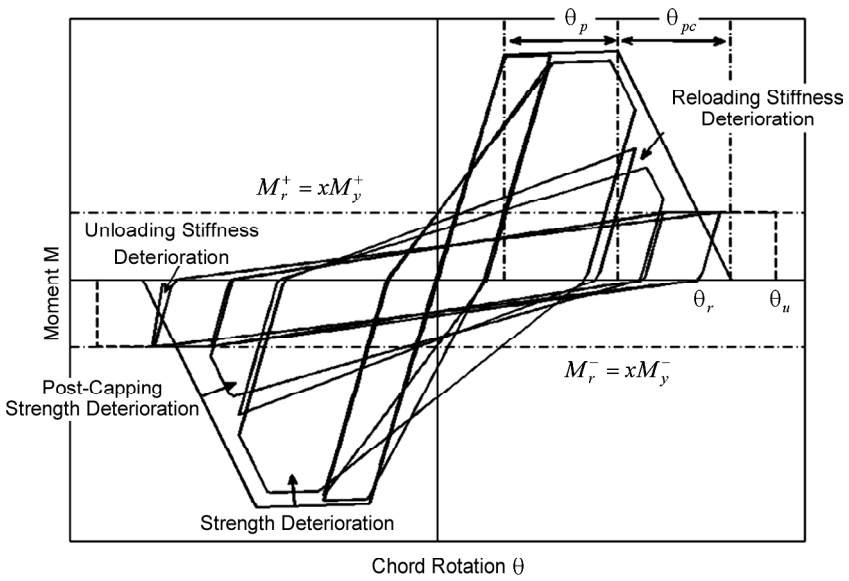

Figure 3. Hysteretic model of RC elements with stiffness and strength degradation [33].

regression analyses on extensive experimental test data, and that, all sources of strength and stiffness degradations have been captured in the tests, it is not required to model the beam-columns joints and bar slip effects explicitly. Thus, the building model was created using center-to-center frame elements with concentrated nonlinear springs located at the two ends of each frame element. Geometric nonlinearities including the global P-*D* as well as the local p-delta effects were considered in the model utilizing co-rotational formulation [34].

Mass properties of the structure were modeled using concentrated mass elements at the nodes. Nodal masses were assigned such that the desired 30% plan CM-CR eccentricity could be achieved. Damping was considered as of Rayleigh mass and stiffness proportional type based on the recommendations in Zareian and Medina [36]. It is interesting to note that, with the advent of the parallel version of the OpenSees analytical platform [34], high-speed nonlinear time-history analyses of the building was possible on a multi-core PC.

4.3. Pushover Analysis Results

Pushover analysis was performed on the structure in both plan directions to examine its overall response up to the point of global instability (collapse) according to recommendations outlined in ASCE/SEI 41-06 [37]. Figure (4) depicts the pushover curves of the structure in both plan X and

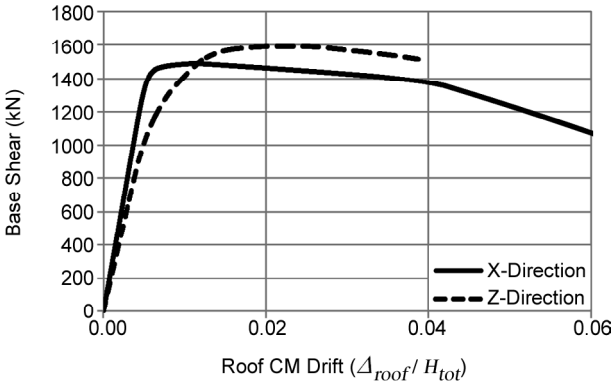

Figure 4. Pushover curves of the structure.

Z-directions with the control node being the center of mass (CM) of the roof. Significant differences are evident between the curves that are directly attributable to the high plan irregularity of the structure and the strong coupling effects of translational and torsional responses. Differences are especially evident in the elastic stiffness, lateral load capacities, structure yield and ultimate achievable drift that altogether affect the structural properties such as "elastic periods of vibrations", "peak strength", "structural over-strength" and "period-based ductility" factors. During the analysis steps, the Z-direction pushover curve stopped at a drift value approximately equal to 3.8% due to shear failure in the columns on the "soft side" frames of the plan. Decreasing of the ductility of the structure is evident for the Z-direction response of the structure due to severe torsional adverse effects.

4.4. Incremental Dynamic Analysis (IDA) Results

The key step of the evaluation procedure is to perform nonlinear dynamic analysis of the structure in both directions under a set of records with varying intensities. This analysis procedure is commonly termed as "incremental dynamic analysis (IDA)" [7].

For both *X* and *Z* plan directions, the procedure outlined in FEMA P-695 [28] was utilized for scaling-up the records. In that procedure, record scaling involves two steps. First, individual records in each set are normalized by their respective peak ground velocities. This step is intended to remove unwarranted variability between records due to inherent differences in event magnitude, distance to source, source type and site conditions, without eliminating overall record-to-record variability. In the second step, normalized ground motions are collectively scaled to specific ground motion intensity such that the median spectral acceleration of the records set matches the spectral acceleration at the fundamental period, T, of the model that is being analyzed. The first step has been performed as part of the ground motion development process in FEMA-P695, so the record sets contained in FEMA-P695 already contain this normalization. The second step is performed as part of the nonlinear dynamic analysis procedure.

For scaling purposes, in this study, the geometric mean (GM) of periods of vibrations in orthogonal directions ($T_{GM} = \sqrt{T_x . T_z}$) was used along with the geometric mean (GM) of strong and weak components spectra of all ground motions in the records set. Then, the scaling factor was calculated for each desired spectral intensity on the median GM spectrum at T_{GM}. At the end, the calculated scaling factor was applied to both strong and weak components of all ground motion records. Table (1) shows the ground motion records used in this example. Selected from FEMA P-695 [28], all have been picked up from PEER NGA online database [38]. This set of records includes various ground motions normalized based on their PGVs and the normalization procedure per FEMA P-695. They are all considered to be far field records. Strong components of the records were applied in the Z-direction while the weak components were placed along the X-direction of the plan. In Figure (5), the median pseudo-acceleration response spectra of all records for both strong and weak components are shown with the median of the geometric mean of both components of all ground motions.

Table 1. Ground Motion records used for the example problem.

ID No.	Record ID	Records IDs According to PEER NGA Database [38]		PGA [m/s^2]
		Component 1	*Component 2*	
1	953	NORTHR/MUL009	NORTHR/MUL279	0.52
2	960	NORTHR/LOS000	NORTHR/LOS270	0.48
3	1602	DUZCE/BOL000	DUZCE/BOL090	0.82
4	1787	HECTOR/HEC000	HECTOR/HEC090	0.34
5	169	IMPVALL/H-DLT262	IMPVALL/H-DLT352	0.35
6	174	IMPVALL/H-E11140	IMPVALL/H-E11230	0.38
7	1111	KOBE/NIS000	KOBE/NIS090	0.51
8	1116	KOBE/SHI000	KOBE/SHI090	0.24
9	1158	KOCAELI/DZC180	KOCAELI/DZC270	0.36
10	1148	KOCAELI/ARC000	KOCAELI/ARC090	0.22
11	900	LANDERS/YER270	LANDERS/YER360	0.24
12	752	LOMAP/CAP000	LOMAP/CAP090	0.53
13	767	LOMAP/G03000	LOMAP/G03090	0.56
14	1633	MANJIL/ABBAR--L	MANJIL/ABBAR--T	0.51
15	721	SUPERST/B-ICC000	SUPERST/B-ICC090	0.36
16	725	SUPERST/B-POE270	SUPERST/B-POE270	0.45
17	829	CAPEMEND/RIO270	CAPEMEND/RIO360	0.55
18	1244	CHICHI/CHY101-E	CHICHI/CHY101-N	0.44
19	1485	CHICHI/TCU045-E	CHICHI/TCU045-N	0.51
20	68	SFERN/PEL090	SFERN/PEL180	0.21
21	125	FRIULI/A-TMZ000	FRIULI/A-TMZ270	0.35

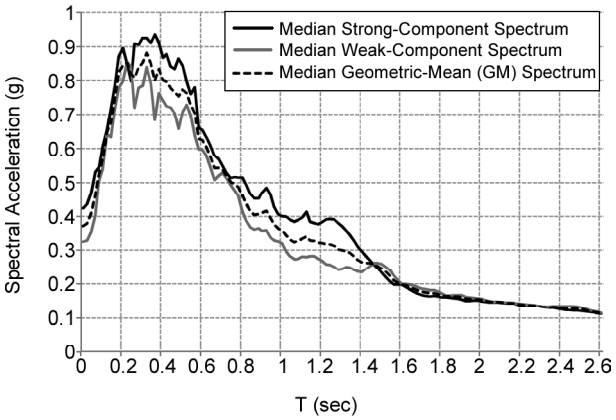

Figure 5. 5% damped median pseudo-acceleration response spectra of all records for both strong and weak components and the median spectrum of the geometric mean of both components spectra of all ground motions.

Results of such bi-directional IDA were combined to obtain the maximum SRSS inter-story drift responses vs. the GM combination of both directions spectral intensities For each ground motion, IDA was continued until one of the "collapse criteria" considered in this study was met. Three collapse criteria including flattening the IDA curve, exceeding maximum SRSS inter-story drifts by 10% and premature elements (primarily columns) failure (elements failure limit states) were examined for each analysis case.

Figures (6-a), (6-b) and (6-c) respectively depicts the maximum X-direction inter-story Drifts vs. S_{a-X}, maximum Z-direction inter-story Drifts vs. S_{a-Z}, and maximum SRSS of inter-story Drifts vs. S_{a-GM} for all ground motions with the median curves overlaid in black.

The authors found that detecting the collapse-level spectral intensity for 3D structures would be possible more conveniently using $D_{\max-SRSS}$ vs. S_{a-GM} data rather than considering $(S_{a-X}, D_{\max-SRSS})$ and $(S_{a-Z}, D_{\max-SRSS})$ pairs separately or $(S_{a-X}, S_{a-Z}, D_{\max-SRSS})$ triples. Note that $(S_{a-X}, S_{a-Z}, D_{\max-SRSS})$ triples are plotted in Figure (9) in the following pages. Flat lines correspond to the S_{a-GM} intensity levels at which the collapse of the structure has occurred. Collapse-level intensities will be used below to calculate the probability of collapse (and no-collapse) conditional on S_{a-GM}.

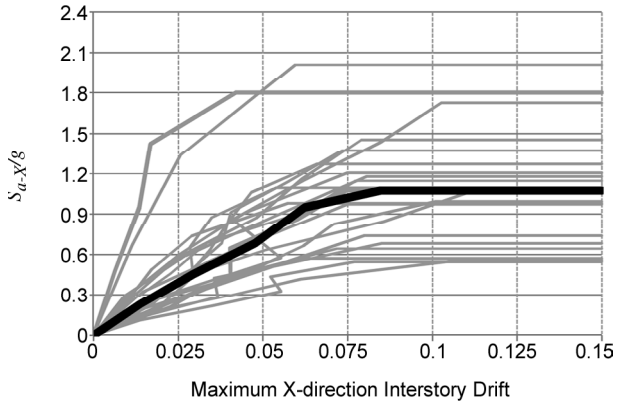

Figure 6a. Maximum X-direction Inter-story Drifts vs. $S_{a\text{-}X}$.

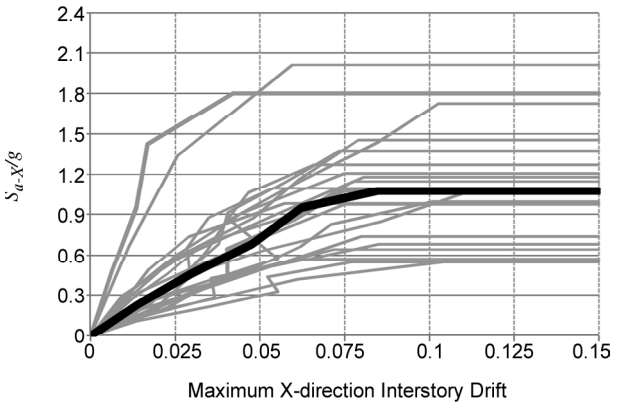

Figure 6b. Maximum Z-direction Inter-story Drifts vs. $S_{a\text{-}Z}$.

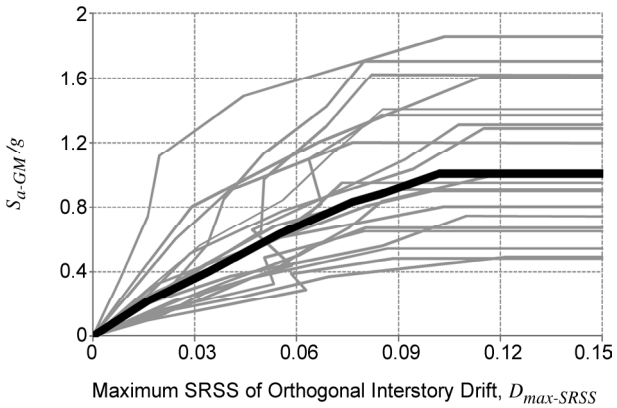

Figure 6c. Maximum SRSS of Inter-story Drifts vs. $S_{a\text{-}GM}$.

5. Probability of No-Collapse and Collapse at Any IM Level

As mentioned in the derivations of the previous sections, for calculating the annual rate of SRSS drift exceedance using the disaggregation technique, probability of no-collapse, namely, $P_{NCL|\,S_a}$ the probability $1-P_{NCL|\,S_a}$, of collapse have to be estimated at various IM levels. For this structure, collapse intensity levels were found according to

the results of incremental dynamic analyses, Figure (6-c), for each record by accounting for the collapse criteria mentioned before. Then, assuming a log-normal distribution of the collapse spectral acceleration [28], a continuous log-normal cumulative density function (CDF) curve was fitted to all available 21 collapse data points. Figure (7) depicts the cumulative density of collapse data points with the fitted CDF curve. The curve is also referred to as the "fragility curve" of the structure. The plot essentially gives the "$1-P_{NCL|\,S_a}$" term at each $S_{a-GM}=\sqrt{S_{a-GX}.S_{a-Z}}$) intensity level.

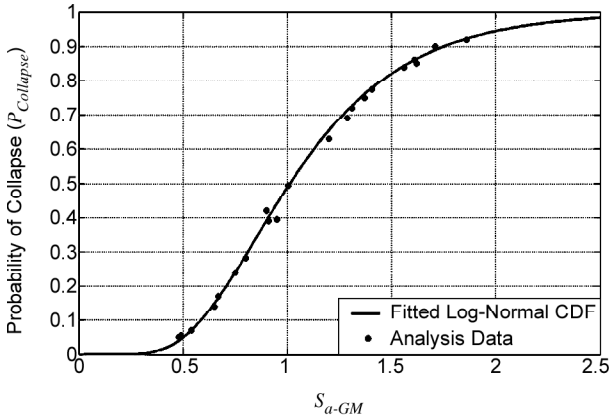

Figure 7. Fragility curve of the structure (probability of collapse vs. $S_{a-GM}=\sqrt{S_{a-X}.S_{a-Z}}$.

6. Calculation of Seismic Hazard Surface Using Deaggregation Procedure

The sample structure is assumed to be located in a far-field site in California (California was selected because seismic hazard deaggregation results are available via the online interactive computer program accessible from the USGS website) on NEHRP soil type D. As stated before, in this study, average of three GMPEs available in NGAW program (PEER [38]) with equal weights, namely the Abrahamson and Silvia [14], Boore and Atkinson [22] and Campbell and Bozorgnia [23] have been used for calculating the scalar term of the seismic hazard deaggregation.

Deaggregating procedure, as discussed, was performed using USGS online interactive computer program which is available for the state of California. It should be noted that, the USGS outputs are available at specific discrete values of spectral periods. Since deaggregation results were not available exactly for $T=1.87$ sec. and $T=0.96$ sec., the authors used the available results for $T=2.0$ sec. and $T=1.0$ sec., respectively. Thus, USGS needs to provide deaggregation results for more spectral periods to be fully applicable in engineering practice. Figure (8) shows the stem plot of joint mean annual rate (MAR) of $S_{(a-X)}$ and $S_{(a-Z)}$ calculated using Eq. (6). The calculated joint seismic hazard surface will be utilized in the next section to calculate the probabilistic seismic demand analysis of the example problem.

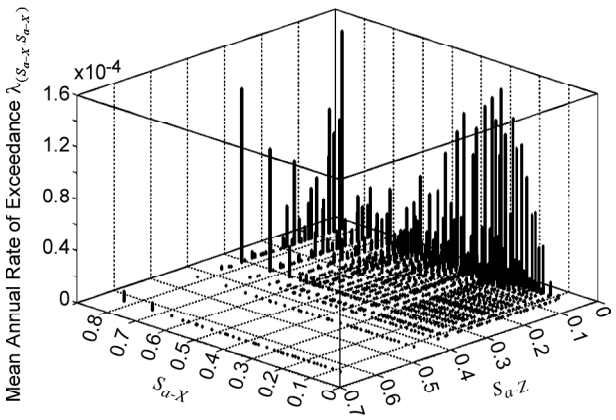

Figure 8. Stem plot of joint mean annual rate (MAR) of equaling seismic hazard S_{a-X} and S_{a-Z}.

7. Calculation of Drift Hazard Curve

In this section, drift demands of the 3D example structure will be estimated according to the SRSS-based probabilistic formulation presented before. As mentioned in previous sections, it is assumed that the SRSS drift data follow a Gaussian log-normal distribution with the "mean value" equals to $\overline{D_{\max-SRSS}}$ and "standard deviation" (dispersion) equals to $\beta_{D_{\max-SRSS}}$. Both of these parameters can be estimated from regression analysis on all maximum SRSS drift data points. Therefore, a regression analysis on median $\ln \overline{D_{\max-SRSS}}$ vs. both $\ln S_{a-X}$ and S_{a-X} is needed. Figure (9) shows all SRSS drifts points vs. S_{a-X} and S_{a-Z} along with the fitted plane.

Using standard regression procedures, a polynomial two-variable function is fitted to natural logarithmic of all triples. Eq. (15) shows the fitted polynomial. The coefficient of determination (R^2) of the fitted function at 95% confidence bounds is 0.6236.

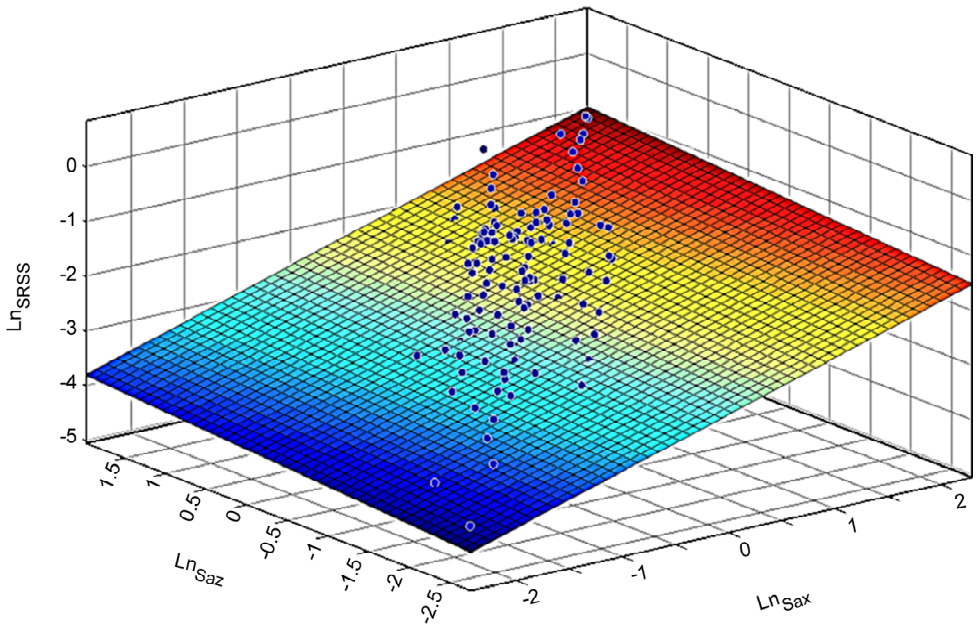

Figure 9. Scatter plot of $\ln(D_{\max-SRSS})$ vs. $\ln(S_{aX})$ and $\ln(S_{aZ})$ with the fitted plane.

$$\ln \overline{D_{\max-SRSS}} = 0.5987\ln S_{a-Z} + 0.114\ln S_{a-X} - 2.578 \quad (15)$$

Now, all the elements required for calculating the drift hazard curve are available. For simplicity, the standard deviation (dispersion) of median SRSS drift values conditioned on $S_{aX}, S_{aZ}(\beta_{D_{\max-SRSS}})$ is assumed to be of constant value of 0.40 for this example based on evaluating dispersion of $D_{\max-SRSS}$ at different levels of spectral acceleration (S_{aX}, S_{aZ}) pairs and judgment made by the authors.

By estimating $\ln \overline{D_{\max-SRSS}}$ from Eq. (15) and $\beta = 0.4$, the following Equation gives the log-normal uni-variable Gaussian CCDF [10]:

$$F^{C}_{D_{\max-SRSS}}(\overline{D_{\max-SRSS}} \mid x,z) = 1-F\left(\frac{\ln D - \ln D_{\max-SRSS}}{\beta}\right) = 1-F\left(\frac{\ln D - 0.5987\ln S_{a-Z} - 0.114\ln S_{a-X} + 2.578}{0.40}\right) \quad (16)$$

Note that in Eq. (16), D represents the maximum SRSS drift demand of the structure.

Substituting the above-calculated $F^{C}(.)$, the estimated $P_{CL|\,S_{a-GM}}$ (and $P_{NCL|\,S_{a-GM}}$) from values extracted from Figure (7), and $\ln \overline{D_{\max-SRSS}}$ from Eq. (15) into Eq. (9) yields:

$$\lambda_{EDP}(D) \cong \sum_{all\ x}\sum_{all\ z}\left\{\left[1-F\times\left(\frac{\ln D - 0.5987\ln S_{a-Z} - 0.114\ln S_{a-X} + 2.578}{0.40}\right)\right]P_{NCL|\,S_{a-GM}} + \left[1-_{NCL|\,S_{a-GM}}\right]\right\}\times P(S_{aZ}=z \mid S_{aX}=x)\times|D\lambda_{SaX}(x)| \quad (17)$$

Recall that the $P(S_{aZ}=z \mid S_{aX}=x)\times|D\lambda_{SaX}(x)|$ product is the joint seismic hazard function of the site which was calculated before, Figure (8).

Figure (10) shows the drift hazard curve (the solid curve) of the structure derived using Eq. (17) and the data specific to the example. For comparison, the drift hazard curve was also calculated without considering the collapse region of nonlinear response (i.e. excluding the P_{NCL} and P_{CL} in Eq. (17)). This curve is depicted in Figure (10) (the dashed curve). It is clearly observed that taking the collapse region of nonlinear response into account affects the mean annual rate of exceedance a specific SRSS drift value significantly and thus represents the seismic demand of the structure more accurately. As it is observed, assessing the seismic demands of the structure based on the hazard drift hazard curve of Figure (10) is similar to assessing such demands in 2D structures. The resulting drift hazard curve is appealing from

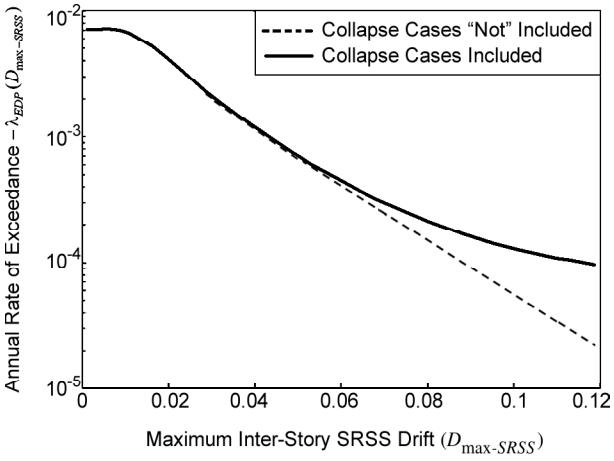

Figure 10. Probabilistic seismic drift demands of the structure (drift hazard curves).

practical points of view. This concludes the example.

In practical applications, however, the user may generally need to assess the $\lambda_{EDP}(D)$ two times: first when the strong component of the ground motion is placed in z-direction, and second when the weak component of the ground motion is placed in z-direction, and then calculating the SRSS drift hazard curves two times. The worst case will govern the design. This is not, however, needed for the highly irregular example structure of this paper; since the z-direction frames control the response due to the severe torsional effects and large $P-D$ demands on these frames.

8. Conclusions

A practical procedure was presented to assess seismic demands of three-dimensional structures considering the collapse region of nonlinear response in a probabilistic framework. The procedure essentially utilizes vector-valued intensity measures based on the two horizontal components of the ground motion spectral intensities at the fundamental modal periods in both principle directions of the structure. The procedure of calculating the drift hazard curve of the structure was developed based on a vector-valued representation of seismic hazard considering both components of horizontal ground motion along with the scalar SRSS combination of horizontal components of inter-story drift values as the demand parameter. The procedure was applied to a plan-asymmetric three-dimensional structure with highly correlated seismic responses in both orthogonal directions under the effects of a far-field record set of ground motions in a step-by-step example. The example demonstrated the efficiency of the proposed method for practical probabilistic evaluation of real structures.

Acknowledgement

The authors would like to acknowledge Dr. Seyed Mehdi Mousavi for his useful comments on the manuscript.

References

1. Jalayer, F. (2003) *Direct Probabilistic Seismic Analysis: Implementing Nonlinear Dynamic Assessments*. Ph.D. Dissertation, Department of Civil and Environmental Engineering, Stanford University, Stanford, California.

2. Baker, J.W. and Cornell, CA. (2005) A Vector-Valued Ground Motion Intensity Measure Consisting of Spectral Acceleration and Epsilon. *Earthquake Engineering and Structural Dynamics*, **34**, 1193- 1217.

3. Zareian, F. and Krawinkler, H. (2009) *Simplified Performance Based Earthquake Engineering*. John A. Blume Earthquake Engineering Center, Technical Report No 169, Department of Civil Tall Engineering, Stanford University, Stanford, California.

4. Jayaram, N. and Baker, J.W. (2009) Correlation model for spatially-distributed ground-motion intensities. *Earthquake Engineering and Structural Dynamics*, **38**(15), 1687-1708.

5. Baker, J.W. (2005) *Vector-Valued Ground Motion Intensity Measures for Probabilistic Seismic Demand Analysis*. Ph.D. Dissertation, Department of Civil and Environmental Engineering, Stanford University, Stanford, California.

6. Barbosa, A.R. (2011) *Simplified Vector-Valued Probabilistic Seismic Hazard Analysis and Probabilistic Seismic Demand Analysis: Application to the 13-Story NEHRP Reinforced Concrete Frame-Wall Building Design Example*. Ph.D. Dissertation, Department of Civil and Environmental Engineering, University of San Diego, San Diego, California.

7. Vamvatsikos, D. and Cornell, C.A. (2001)

Tracing and Post-Processing of IDA Curves: Theory and Software Implementation. Report No. RMS-44, RMS Program, Stanford University, Stanford.

8. Faggella, M. Barbosa, A.R., Conte, J.P., Spacone, E., and Restrepo, J.I. (2013) Probabilistic seismic response analysis of a 3-D reinforced concrete building. *Journal of Structural Safety*, **44**, 11-27.

9. Gehl, P., Seyedi, D., and Douglas, J. (2013) Vector-valued fragility functions for seismic risk evaluation. *Bulletin of Earthquake Engineering*, **11**(2), 365-384

10. Kottegoda, N.T. and Rosso, R. (2008) *Applied Statistics for Civil and Environmental Engineers*. 2nd Edition, Blackwell Publishing.

11. Shome, N. and Cornell, C.A. (1999) *Probabilistic Seismic Demand Analysis of Nonlinear Structures*. Report No. RMS-35, RMS Program, Stanford University, Stanford.

12. Ambraseys, N.N. and Douglas, J. (2003) *Near-field horizontal and vertical earthquake ground motions. Journal of Soil Dynamics and Earthquake Engineering*, **23**, 1-18.

13. Bozorgnia, Y. and Bertero, V. (Editors) (2004) *Earthquake Engineering: From Seismology to Performance-Based Seismic Engineering*. CRS Press.

14. Abrahamson, N.A. and Silva, W.J. (2008) Summary of the Abrahamson and Silva NGA ground motion relations. *Earthquake Spectra*, **24**, 67-97.

15. Bazzurro, P. (1998) P*robabilistic Seismic Demand Analysis*. Ph.D. Dissertation, Dept. of Civil and Environmental Engineering, Stanford University, Stanford, California.

16. Bazzurro, P. and Cornell, C.A. (2002) Vector-valued probabilistic seismic hazard analysis (VPSHA). *Proceedings of 7th U.S. National Conference on Earthquake Engineering (7NCEE)*, Urban Earthquake Risk, Boston, Massachusetts, USA. Oakland, California: Earthquake Engineering Research Institute.

17. Baker, J.W. and Cornell, CA. (2006) Correlation of response spectral values for multi-component ground motions. *Bulletin of the Seismological Society of America*, **96**(1), 215-227.

18. Stewart, J.P., Abrahamson, N.A., Atkinson, G.M., Baker, J.W., Boore, D.M., Bozorgnia, Y., Campbell, K.W., Comartin, C.D., Idriss, I.M., Lew, M., Mehrain, M., Moehle, J.P., Naeim, F., and Sabol, T.A. (2011) Representation of bidirectional ground motions for design spectra in building codes. Earthquake Spectra, **27**(3), 927-937.

19. Ni, Sh.H., Zhang, D.-Y., Xie, W.-Ch., and Pandey, M.D. (2012) Vector-valued uniform hazard spectra. *Earthquake Spectra*, **28**(4), 1549-1568.

20. Doornik, J.A. and Hansen, H. (1994) An omnibus test for univariate and multivariate normality. Discussion Paper W4&91. Nuffield College, Oxford, UK.

21. Henze, N. and Wagner, Th. (1997) A new approach to the BHEP tests for multivariate normality. *Journal of Multivariate Analysis*, **62**, 1-23.

22. Boore, D.M., and Atkinson, G.M. (2008) Ground-motion prediction equations for the average horizontal component of PGA, PGV, and 5%-damped PSA at spectral periods between 0.01 s and 10.0 s. *Earthquake Spectra*, **24**, 99-138.

23. Campbell, K.W. and Bozorgnia, Y. (2008) Campbell-Bozorgnia NGA horizontal ground motion model for PGA, PGV, PGD and 5% damped linear elastic response spectra. *Earthquake Spectra*, **24**, 139-171.

24. Baker, J.W. and Jayaram, N. (2008) Correlation of spectral acceleration values from NGA ground motion models. *Earthquake Spectra*, **24**(1), 299-317. DOI: 10.1193/1.2857544

25. United States Geological Survey (USGS) (2014) 2008 NSHMP PSHA Interactive Deaggregation. at www.geohazards.usgs.gov/deaggint/2008.

26. International Building Code (IBC) International building code council (2009).

27. ACI (2011) Building Code Requirements for

Structural Concrete (ACI 318-11) and Commentary (ACI 318R-11), American concrete Institute, Farmington Hills, Michigan.

28. FEMA P695. (2009) Quantification of Building Seismic Performance Factors. Report No. P695, Federal Emergency Management Agency, Washington, D.C.

29. Zareian, F. and Krawinkler, H. (2007) Prediction of collapse-how realistic and practical is it, and what can we learn from it? *The Structural Design of Tall and Special Buildings*, **16**(5), 633-653.

30. Haselton, C.B. (2006) *Assessing Seismic Collapse Safety of Modern Reinforced Concrete Moment-Frame Buildings*. Ph.D. Dissertation, Department of Civil and Environmental Engineering, Stanford University, Stanford, California.

31. Ibarra, L.F., Medina, R.A., and Krawinkler, H. (2005) Hysteretic models that incorporate strength and stiffness deterioration. *International Journal for Earthquake Engineering and Structural Dynamics*, **34**(12), 1489-1511.

32. Panagiotakos, T.B. and Fardis, M.N. (2001) Deformations of reinforced concrete members at yielding and ultimate. *ACI Structural Journal*, **98**(2), 135-148

33. Ibarra, L.F. and Krawinkler, H. (2005) *Global Collapse of Frame Structures Under Seismic Excitations*. PEER Report 2005/06, and John A. Blume Earthquake Engineering Center Technical Report No 152, Department of Civil tall Engineering, Stanford University, Stanford, California.

34. OpenSees (2012) Open System for Earthquake Engineering Simulation, Pacific Earthquake Engineering research Center, University of California, Available at http://opensees.berkeley.edu.

35. Manie, S. and Moghadam, A.S. (2012) Experiences acquired through nonlinear modeling analyzing structure for collapse assessment. *15th World Conf. on Earthquake Engineering*, Lisbon, Portugal, 1596.

36. Zareian, F. and Medina, R. (2010) A practical method for proper modeling of structural damping in inelastic plane structural systems. *Journal of Computers and Structure*, **88**, 45-53

37. ASCE (2007) *Seismic Rehabilitation of Existing Buildings*. ASCE Standard ASCE/SEI 41-06, American Society of Civil Engineers, Reston Virginia.

38. PEER. (2012) PEER NGA Database. Pacific Earthquake Engineering Research Center, University of California, Berkeley, California, Available at http://peer.berkeley.edu/nga/.

?. Baker, J.W. and Cornell, C.A. (2008) Vector-valued intensity measures incorporating spectral shape for prediction of structural response. *Journal of Earthquake Engineering*, **12**(4), 534-554.

?. Faouzi, Gh. and Nasser, L. (2013) Scalar and vector probabilistic seismic hazard analysis: application for Algiers City. *Journal of Seismology, Springer*. DOI 10.1007/s10950-013-9380-5

?. Fardis, M.N. (Editor) (2009) *Seismic Design, Assessment and Retrofitting of Concrete Buildings Based on EN-Eurocode 8*. Springer.